Available online at www.sciencedirect.com
SCIENCE DIRECT®

ELSEVIER

Optical Fiber Technology 12 (2006) 122–147

Optical Fiber Technology

www.elsevier.com/locate/yofte

Optical spectral broadening and supercontinuum generation in telecom applications

S.V. Smirnov [a], J.D. Ania-Castanon [b,*], T.J. Ellingham [b], S.M. Kobtsev [a], S. Kukarin [a], S.K. Turitsyn [b]

[a] *Laser Systems Laboratory, Novosibirsk State University, Pirogova 2, Novosibirsk-90, 630090 Russia*
[b] *School of Engineering and Applied Science, Aston University, Aston Triangle, Birmingham B4 7ET, UK*

Received 11 April 2005; revised 13 July 2005

Available online 1 September 2005

Abstract

We overview the recent development in applications of spectral broadening and supercontinuum generation in the field of optical communications. Special attention is dedicated to recent results obtained in our research groups.

Keywords: Nonlinear spectral broadening; Supercontinuum generation; Raman amplification; Dual-core tapered fiber

1. Introduction

The spectral broadening of a coherent or partially coherent light signal in optical fibers has captured much attention in recent years, fuelled by the advent of microstructured photonic crystal fibers (PCF) presenting a very high nonlinear response [1,2], and thanks to its multiple practical applications, both within and outside the field of optical communications [3–11]. The growing interest to this phenomenon has led to a steady progress in the understanding of the interplay between the different nonlinear processes affecting high power radiation evolution in the optical fiber waveguide. By applying techniques such

* Corresponding author.
E-mail addresses: smirsv@ngs.ru (S.V. Smirnov), aniacajd@aston.ac.uk (J.D. Ania-Castanon).

1068-5200/$ – see front matter
doi:10.1016/j.yofte.2005.07.004

as frequency-resolved optical gating (FROG) [12–15] and spectral-phase interferometry for direct electric-field reconstruction (SPIDER) [16–19], researchers have been able to analyze nonlinearly-broadened radiation to a degree never achieved before, improve on the models used to describe the broadening process and increase our understanding of the phenomenon [20–27]. From a purely practical point of view, the progress has also been impressive, and has allowed, for example, for the generation of supercontinuum (SC) radiation with spectral widths in excess of the several hundreds nanometers [28–31] in microstructured, tapered and highly-nonlinear fibers (HNLF). Supercontinuum generation, first observed in 1970 by Alfano and Shapiro in bulk borosilicate glass [32], is an essentially nonlinear phenomenon, product of the synergy between several fundamental nonlinear processes; most important of them are self-phase modulation (SPM), four-wave mixing (FWM) and stimulated Raman scattering (SRS). The interplay between different nonlinear effects affects important SC properties such as homogeneity and coherence. The interaction between different nonlinear processes is determined by the pumps' spectral locations and powers, and the nonlinear and dispersive characteristics of the medium. Recent progress in the development of PCFs offers interesting opportunities to control (to some extent) SC generation by using specially designed fiber waveguides with desirable dispersive and nonlinear properties [33]. Large spectral broadening and SC in optical fiber at telecom wavelengths was first demonstrated in [34,35]. Application of photonic crystal fiber for SC generation was demonstrated in 1999 in [36,37].

Despite recent advances in SC studies, there are a number of fundamental problems to be studied, and a full understanding as well as a proper modelling of the phenomenon are yet to be achieved. Some of the current tendencies for basic research on the field include the study of the noise and coherence properties [25,26,38–42] of SC, and the analysis of the effect of polarization [43,44] in the nonlinear broadening process, to name a few.

A healthy fraction of the current research is focused on the applications of spectrally broadened radiation, whether in bio-medical optics, where it allows the improvement of longitudinal resolution in optical coherence tomography by more than an order of magnitude [7,9–11,45–48]; in optical frequency metrology, where a revolutionary break-through has been achieved [3–6,49–54]; or in many other areas from material science [55] to telecommunications. Note that in some telecom applications, as opposed to the technologies mentioned above, the ultra-large broadening corresponding to SC generation is not a desirable feature at all, and many useful applications require moderate or even minimal spectral broadening of the signal or e.g., pumping wave. The aim of this manuscript is to provide the reader with a general overview of the recent development of spectral broadening applications and SC generation in the particular area of optical communications. We would like also to point out that the main emphasis in this paper will be made on the overview of the results obtained in our groups, and it is not our intention here to cover comprehensively all the fast growing field of SC generation research.

2. Basic physics of optical spectral broadening and SC generation in fibers

Light radiation propagating through a nonlinear medium experiences spectral broadening that could be very substantial (up to two octaves or even more) under certain conditions.

The SPM-effect caused by the dependence of the refractive index on the intensity of the transmitted light (Kerr nonlinearity)—has been identified in the early works on continuum generation (CG) of 4-ps-long laser pulses propagated through bulk samples of different glasses and crystals [32,56] as the main mechanism responsible for generation of ∼50-THz-wide spectra. In a medium with Kerr nonlinearity, after propagation over the distance z, an optical pulse acquires an additional phase (due to the nonlinear part Δn of the refractive index) that can be estimated [57] as

$$\phi_{\mathrm{NL}}(z,t) = \Delta n \frac{\omega}{c} z = n_2 I(t) \frac{\omega}{c} z. \tag{1}$$

The corresponding frequency shift is

$$\delta\omega(z,t) = -\frac{d}{dt}\phi_{\mathrm{NL}}(z,t) = -n_2 \frac{dI(t)}{dt}\frac{\omega}{c} z, \tag{2}$$

where n_2 is the nonlinear refractive index of the medium, ω is the carrier frequency, c is the light speed in vacuum, and I is the power flux density. It can be seen from (2) that, as the optical pulse propagates the frequency at its leading edge decreases and that at the trailing edge it increases. Spectral broadening is proportional both to the energy flux and to the propagation distance; therefore, SPM can be amplified due to self-trapping, which was reported in [56]. When the pump power is greater or about 10 $\mathrm{TW/cm^2}$, which can be reached in light filaments, free-electron plasma formation can also occur, further strengthening the effect of SPM [58].

One of the primary inherent disadvantages of CG schemes based on bulk media (also including those based on liquids [59,60] and gases [61–63] as nonlinear media) is the requirement of high pump powers. Typical level of power density required is around several terawatts per $\mathrm{cm^2}$, thus necessitating additional amplification of laser pulses at the risk of sample damage. It became possible to alleviate such high pump power requirements during the next phase of SC generation studies using optical fibers as nonlinear medium [20,64–66]. The required pump power was lowered, on the one hand, due to a substantially longer path of the interaction between light and matter, and on the other hand, thanks to a higher localization of radiation. Thus, for example, the dispersion length for 4-ps-long Gaussian pulses at 530 nm in standard SMF-28 is about 80 m, being 5.3×10^4 times larger than the length of light filaments observed in [56], which amounted to about 1.5 mm. The effective area of SMF-28 at 530 nm is about 50 $\mu\mathrm{m}^2$, which is 30–60 times less than the area of the power concentration estimated for 5–10 light filaments having a diameter of 20 μm each as observed in [56]. Correspondingly, the generation of continuum covering a significant part of the visible spectrum became possible with a peak pump power of only 1 kW [64], whereas the power used to induce CG in glasses was about 200 MW [56].

In early experiments exploiting optical fibers [64,65] continuum was formed by broadening and merging of separate spectral lines, generated due to SRS and FWM. Phase matching conditions for the latter were met as a result of multi-mode propagation of light through the fiber. SPM could not contribute considerably to the spectrum broadening because of low power density and comparatively long pulses (within pico- and nanosecond range), so that the value of dI/dt in (2) was small compared to those used in bulk media experiments.

In the next generation of fiber experiments on SC generation, however, SPM plays the key role again, allowing one to obtain flat spectra with good noise parameters in the normal dispersion regime. By using additional optical elements with negative second group velocity dispersion β_2 it is possible to achieve a temporal compression of pump pulses as well [67–69]. With this method, it was possible to generate pulses as short as 6 fs [70]. Another physical mechanism of spectral broadening is based on adiabatic soliton compression in a fiber with decreasing dispersion [20,71–73]. The relative disadvantage of this method is the instability of higher-order solitons in the presence of noise, which imposes an upper limit on the pump power and hence on the resulting spectral width.

One can also combine these two approaches using specially designed fibers with dispersion smoothly changing along the fiber from positive to negative values [72–74].

The most recent period of CG investigations is associated with the development of PCFs [75–83]. Essentially, they consist of quartz fibers sheathed with a conduit formed by a two-dimensional (usually regular) array of air-filled capillaries [84]. It is pertinent to note that there are two different types of fibers called PCF. The first of them proposed in 1996 [75] has a quartz core with refractive index greater than the average refractive index of cladding formed by an array of air capillaries. The principle of light propagation for this type of fiber is similar to that of standard optical fibers where the condition $n_{\mathrm{core}} > n_{\mathrm{cladding}}$ is also met. Fibers of the second type introduced in 1999 [85] have an air channel in the core, so that the inverse inequality holds: $n_{\mathrm{core}} < n_{\mathrm{cladding}}$. These fibers can be considered as two-dimensional crystals and the one or several holes (capillaries) absent in the center of the lattice can be treated as a defect. Light propagation along this type of fiber is possible due to the photon band gap effect. One of the most important applications of hollow-core PCF is in high power lasers as the breakdown threshold of gases is much higher than that of solids [84]. In this paper we will use the term PCF for fibers of the first type—guiding light through the effect of total internal reflection.

Compared to conventional optical fibers PCF features several significant advantages. First of all, this type of fiber gives a quite unique opportunity of dispersion control. This is possible because the penetration of the electromagnetic field into the fiber cladding (and hence, its effective index of refraction) depends on the wavelength of radiation inside the fiber. As a result, the refractive index of the cladding at different wavelength can be controlled by arranging capillaries in a certain way at the time of pulling. This technique was used to create fibers with flat dispersion profile [86–93] which allow generation of flat and wide SC spectra. In addition, one can shift the zero dispersion wavelength λ_{ZD} of PCF and produce anomalous dispersion in the visible spectral region [94,95]. It is the latter feature that made it possible to generate SC spanning more than two-octaves [37]. Another advantage is that PCF can be designed to support only one spatial mode in a wide spectral range [77,82] having rather small effective area of the waveguide mode.

We note also a special type of PCF called free-strand or cobweb fiber [28,96]. The quartz core of such waveguides is attached to the cladding by a cobweb-like structure of thin bridges, from which the name of the fibers comes. Since the core of cobweb fibers is almost entirely surrounded by air, the structure of these waveguides is similar to that of air-clad tapered fibers (ACTF). Continuum spectra generated in these two types of fibers under the same conditions are nearly identical [28]. In particular, CG spanning two-octaves was observed in ACTF [97,98]. Soliton self-frequency shift of several hundred nanometers was also demonstrated in ACTF [99]. ACTF have some advantages such as an easier fabrication process compared to PCF as they can be made by pulling a heated conventional single-mode fiber. On the other hand, the design freedom is limited as there is practically only one single parameter of ACTF that can be controlled—its waist diameter, which means there are limitations on the fabrication of ACTF with the required dispersion characteristics. Besides, it is quite complicated to make long ACTF because of the fragility of very thin quartz strand.

Micro-structured fibers can be designed within a huge range of possible dispersive characteristics and parameters and their nonlinearity can be rather large due to a small effective area. These remarkable features call into play a plethora of nonlinear mechanisms of spectral broadening in PCF that may differ depending on waveguide dispersion profile, power, wavelength and duration of pumping pulses. For example, using femtosecond pump pulses within the anomalous dispersion region, most of the authors point out a key role of soliton effects in CG [100–103]. The red wing of the spectrum generated under these conditions is formed due to soliton self-frequency shift [104–106], while the blue one, is a result of resonant energy transfer and soliton fission. In the case when a femtosecond pump falls within the normal dispersion region CG develops in two stages. First, the spectrum of the pumping pulse is broadened to the point of zero dispersion due to SPM and SRS, then soliton effects come into play [100]. Parametric processes and Raman scattering are also observed to contribute to CG under these circumstances [101].

When the duration of pumping pulses is within the picosecond and nanosecond domain, SPM does not affect CG significantly. Spectral broadening is usually assumed to occur as a result of SRS which generates a series of spectral lines, each of these once emerged can act as a pump source for parametric processes. Phase matching conditions can be met in this case due to vicinity of zero dispersion wavelength [107–109]. When energy is transferred to the region of anomalous dispersion, modulation instability (MI) and soliton effects come into operation and broaden the spectrum further [1,109].

Let us illustrate in more detail the spectral broadening of femtosecond pump pulses propagating in the anomalous dispersion region, this case being the most frequent in CG studies. To do this we will examine the dynamics of spectrum broadening as a function of pump power. Figure 1 shows simulated spectra of chirp-free 60-fs-long $sech^2$ pulses after passing 10 cm through a 2.3-μm-diameter ACTF waist. Pump pulse power increases from 0.5 kW for the bottom graph a up to 20 kW for the top graph f. The pump pulse spectrum is shown in the bottom of the figure with dotted line. Our simulations are based on the generalized nonlinear Schrödinger equation [57] which is mostly used for theoretical modelling of CG when polarization effects can be averaged out or neglected. Continuum spectra given in Fig. 1 are typical for the case of femtosecond pump; similar results can be found in numerous published papers [13,25,107]. When $P_0 = 0.5$ kW (Fig. 1a) the pump pulse spectrum is broadened due to SPM. As the pump peak power reaches 2.5 kW (Fig. 1b) a peak at the long-wavelength side of the spectrum emerges. It corresponds to an optical soliton which experiences an increased shift of its frequency farther into IR region as the pump power grows, thus leading to further spectral broadening. Besides, in this process the number of solitons increases, their spectra begin overlapping and form the red wing of the continuum spectrum. As the pump power rises, the spectrum is also broadened towards shorter wavelengths. The position of the short-wavelength spectrum

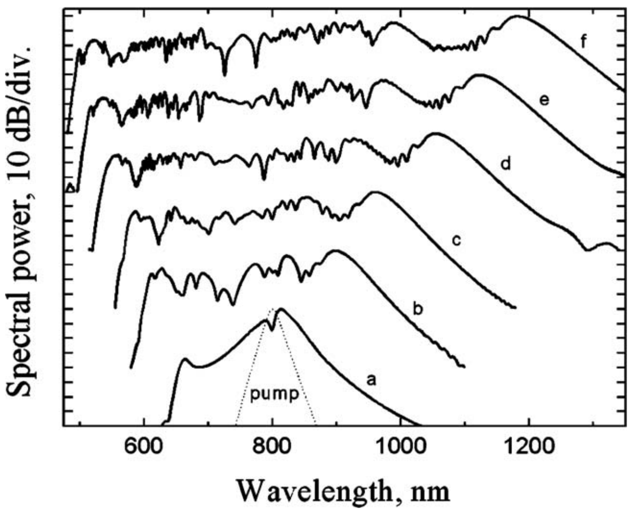

Fig. 1. Simulated spectra at the exit of 10-cm-long tapered fiber waist with diameter of 2.3 µm. We use 60-fs-long sech^2 pump pulses at $\lambda = 800$ nm. Pump peak power is 0.5 kW (for graph a), 2.5 (b), 5 (c), 10 (d), 15 (e), and 20 kW (f). The pump pulse spectrum is shown at the bottom with dotted line.

edge depends on the fiber dispersion and is governed by the equality of temporal delays for long- and short-wavelength components of continuum radiation, which agrees with the model of resonant energy transfer into the short-wavelength part of the spectrum mentioned above.

Reports on observation of spectral broadening in media or with light sources never used before with the purpose of CG constituted a significant part of early papers in this field, and they have not ceased to appear. Among these are, for example, generation of broadband continuum directly in Ti:Sa laser [110,111] and CG in fibers with continuous wave pump [112–115]. However, at the present phase of CG studies papers of another sort are more common. They are dedicated to the investigation of different properties of continuum radiation, such as spectral shape and width [28,74,96,116–118], temporal structure [13,25,116,118–120], polarization [1,96,121], noise and coherence [20,25, 51,96], as well as to research into dependence of these properties on conditions of CG. Aside from this, a considerable number of papers seek to understand physical mechanisms of spectral broadening [1,13,100–103,107,122]. The practical goal of the most of these studies is to optimize continuum generation for diverse applications, every one of which sets its own specific requirements to the SC properties. For instance, the longitudinal resolution of 3D-images collected in optical coherence tomography is inversely proportional to the temporal coherence of a probe radiation, therefore, to obtain more detailed tomograms one should use continuum sources with lower temporal coherence. In order to develop continuum-based universal high-precision optical frequency meters for metrology it is essential that the span of the continuum spectrum be wider than a full octave (i.e., $\omega_{\max}/\omega_{\min} > 2$) and represent an equidistant frequency comb. For utilization of continuum for frequency stabilization and optical clock development, output within the entire spectral range from $\omega_{\min}$ to $\omega_{\max}$ may be unnecessary, so continua with deep spectral gaps or those failing the condition of equidistant frequencies in unused wavelength regions will be quite acceptable. For example, this is the case of self-frequency shifted soliton generation regime; radiation spectra may meet the condition $\omega_{max}/\omega_{min} > 2$, but the question of its coherence remains open [123]. As far as telecom applications are concerned, the spectral flatness and temporal parameters of continuum are of a prime importance in the development of multiplexing schemes for fiber communication systems. Development of broadband Raman fiber amplifiers requires a high degree of spectral uniformity of the gain factor and a continuum with a specific spectral profile $I(\lambda)$ can be used as a pump source to solve this problem in a cost-efficient way, avoiding multi-pump schemes.

3. Application of spectral broadening and continuum generation in telecom

In this section we briefly overview the main applications of the spectral broadening effect and SC generation in optical fiber communications.

3.1. Pulse compression and short pulse generation

Islam et al. [124] demonstrated the application of nonlinear broadening to the generation of femtosecond pulses. When a fiber is pumped in the anomalous dispersion regime with a narrow-spectrum laser, modulation instability and the soliton self-frequency shift initiate a multi-soliton collision that generates a series of short, low intensity solitons. On the other hand, nonlinear temporal compression has been for a long time a well-known technique for generating ultra-short pulses [69,125]. In this technique, the spectrum of the signal is first nonlinearly broadened, and the chirp is then eliminated by a dispersion-compensating element. Südmeyer et al. have recently demonstrated [126] that the use of microstructured fibers, combined with a prism pair for chirp elimination, would make it possible for this method to be applied at very high power levels, obtaining a train of 33 fs pulses with peak power of 12 MW, whereas Schenkel et al. [127] employed gas-filled hollow fibers for the broadening, together with a spatial light modulator using SPIDER measurements as feedback signal acting as the dispersive element, to generate 3.8 fs pulses with estimated energies up to 15 μJ.

The fundamental limits for the generation of few-cycle pulses from compression of SC spectra generated in microstructured fiber have been analyzed by Dudley et al. [128], confirming that the compressed pulse quality was closely related to the spectral coherence of the SC. According to their work, a median coherence of about 0.7 could be expected to be a good benchmark for the potential compressibility of SC to few-cycle pulses, provided compressors with high enough resolution to compensate for the fine structure in the SC group delay would be made available in the future.

Conversely, high-power ultra-short pulse sources obtained with techniques such as the ones explained above can be used as the input to generate ultrabroadband octave-spanning SC radiation in optical fiber, as illustrated, for example, by the works of Nishizawa et al. [31,129]. Stretched femtosecond pulses have been used by Nicholson et al. [130] in the development of a high repetition rate, swept-wavelength Raman pump source.

3.2. Multi-wavelength optical sources

One of the most important applications of SC to the field of telecommunications is the design of multi-wavelength sources for ultra-broadband wavelength-division-multiplexed (WDM) systems based on spectral slicing of SC generated by a single laser. As mentioned in Section 3.1, a powerful short optical pulse can be nonlinearly broadened into a SC spectrum. This spectrum can then be sliced in an array of filters to create a series of WDM channels. This was the approach originally adopted by Morioka et al. [66] using short (few ps) pulses with GHz repetition rates in dispersion-decreasing fiber (DDF) to create WDM pulsed sources, and different variations have been implemented by multiple authors [131–133] ever since.

The ultimate limit for dense packing of WDM channels in a SC generated from a pulsed source is imposed by the spectral distance between cavity modes in the original mode-locked laser. In a medium with normal dispersion, the cascaded nonlinear processes used to broaden the spectrum preserve the structure of cavity modes [134] present in the original laser output. This makes possible to generate an ultra-broad frequency comb, in which the separation between peaks corresponds to the microwave modelocking frequency of the source laser, with an accuracy of the order of kHz. Each peak can be considered as potential transmission channel. This property was used by Takara et al. [135] to generate more than 1000 optical frequency channels with a channel spacing of 12.5 GHz between 1500 and 1600 nm. Out of them, between 600 and 700 were demonstrated to offer SNRs and Q-factors sufficient for 2.5 Gbit/s multi-span transmission. Following the same principle, Takara et al. [136] recently reported 124 nm seamless transmission of 3.13 Tbit/s, over 160 km using 313,10 Gbit/s channels spaced 50 GHz. In their experiment they used Raman amplification in hybrid tellurite/silica fiber for improved gain flatness. In an even more recent experiment from the same group, Ohara et al. [137] demonstrated transmission of over 1000 channels, with a 6.25 GHz-spacing, using a SC multi-carrier source. The conservation of coherence properties was also successfully employed by Sotobayashi et al. [138] to create a 3.24 Tb/s (84-channel 40 Gbit/s) WDM source of carrier-suppressed return-to-zero (CS-RZ) pulses. By generating the SC in a normal dispersion fiber, the relative phase between adjacent pulses is preserved in the different channels, allowing for the multiplication of the CS-RZ structure.

SC WDM sources can be of great use in more modest systems: Kartalopoulos et al. [139] recently studied the use of supercontinuum sources in coarse WDM applications with channel protection, and concluded that in systems with a limited number of channels, the use of supercontinuum WDM sources can result in lower costs and increased reliability.

3.3. All-optical analog-to-digital conversion

In a series of recent papers [140–142], Oda et al., proposed and successfully demonstrated a novel quantization scheme for all-optical analog-to-digital conversion based on the splicing of the nonlinearly broadened spectrum of a train of short pulses by means of an arrayed waveguide grating (AWG).

By varying the power of the input pulses by means of an erbium-doped fiber amplifier (EDFA), prior to their launch into a section of dispersion-decreasing fiber (DDF), they were able to generate a series of nonlinearly broadened quasi-symmetrical spectra, in which the degree of broadening was directly dependent on the amount of power injected into the fiber. The broadened spectra were then passed through an AWG providing a series of output ports set in the Stokes side of the initial signal. The number of ports that are "on" (i.e., the number of ports that transmit power above a certain threshold) for each spectrum depend on the amount of broadening, and thus on the power of the input pulses. This imaginative solution, partially based on the work of Ho et al. [143] still has to overcome some important problems, such as the high average power requirements of the first prototype, but could open the door to a new generation of all-optical analog-to-digital convertors. A recent refinement [144] uses a NOLM for the coding of the signal after the slicing. Since the proposed solution relies only on fiber nonlinearity, and not on electronic devices, the scheme can operate beyond 40 GHz.

3.4. TDM-to-WDM-to-TDM conversion

Sotobayashi et al. [145,146] proposed and demonstrated the concept of a photonic gateway able to perform conversion from time-division-multiplexed (TDM) signals to WDM signals and vice-versa by using SC generation. Their scheme is based on combining ultrafast photonic processing in both the time and the frequency domain, using optical gating and time shifting in the time domain, combined with nonlinear broadening under normal dispersion and spectral slicing.

In order to convert from TDM to WDM, the signal is first amplified and then nonlinearly broadened. The spectral properties of SC generated under normal dispersion (high coherence, flat spectrum, easily equalized channel power, similar pulsewidth in different frequencies and relative independence of the spectrum on the input pulse characteristics) allow for the possibility of generating a series of independent channels through spectral splicing, all carrying the same sequence of pulses as the original signal. By time-shifting the different channels, and using an optical time gate with the appropriate repetition rate, it is then possible to split the information between the newly created WDM channels, effectively switching from TDM to WDM.

For the opposite conversion, the process starts by differentially time-shifting the WDM channels, so the bits transmitted at different frequencies are all in temporal sequence. Then, nonlinear broadening allows for the superposition of all the different channels, and spectral splicing selects a single channel at the central frequency, that now contains the complete bit sequence.

The solution, of course, is not without its drawbacks. Although quite robust against input pulse quality and presenting a good noise performance, its response is polarization dependent (because of the time-gating devices) and its application is limited to the return-to-zero format. It is nevertheless an excellent illustration of the possibilities that nonlinear broadening has opened in terms of adding flexibility to signal manipulation.

3.5. Optical fiber characterization

We have already mentioned that nonlinearly broadened radiation can be applied to optical metrology. Measurements of the wavelength-dependent attenuation can be made simultaneously over a wide bandwidth, and group-velocity-dispersion (GVD) measurements in conventional fiber with group delay resolutions of 0.01 ps/km in fiber lengths of up to 130 km over more than 600 nm, using SC white pulses was demonstrated by Mori et al. [147]. GVD measurements can also be carried out in nontypical media such as tapered air–silica microstructure fibers by using white-light interferometry with the help of broadband sources, as demonstrated by Ye et al. [148]. Spectral interferometry with a SC source was also used by Jasapara et al. [149] to perform GVD measurements in photonic bandgap fiber.

4. Design of supercontinuum fiber sources

The SC is a particular form of nonlinearly broadened radiation that preserves the coherence properties of the input source. An important effort has been dedicated to the creation of acceptably compact sources of SC radiation, usually with additional specific properties dependent on the application they are aimed towards, such as increased flatness, high coherence, low noise or a fixed polarization [150–153].

The noise limitations [26] and coherence properties [25] of SC spectra generated in different kinds of fiber have been studied theoretically and experimentally by multiple groups with the goal of designing the best possible SC sources. The effect of pump fluctuations in the generation of SC pulses was first studied by Mori et al. [38], showing that pulses were more stable when generated in dispersion flattened dispersion decreasing fiber (DDF). Nakazawa et al. [39] studied the degradation of coherence during SC generation in DDF, concluding that FWM phase-matched by SPM and a small anomalous dispersion in the presence of amplified spontaneous noise (i.e., modulational instability) was the main cause for the loss of coherence. In more recent times, other studies have appeared about the noise and coherence properties of SC generated in PCF and highly-nonlinear fiber (HNLF) [42,154]. Corwin et al. [26,41] identified the amplification of quantum-limited shot noise and spontaneous Raman scattering as the main sources for amplitude fluctuations in microstructure fiber, and concluded that short input pulses were critical for the generation of broad SC with low noise, whereas Dudley et al. [25] demonstrated that coherence degradation depended strongly on the input pulse duration and wavelength, and that the effect of modulational instability in anomalous dispersion could be reduced by using short pulses. All these and other theoretical and experimental studies that have followed, have contributed to refine the design of potential SC sources.

Being able to produce SC in a particular polarization is not only essential for some applications, but indeed fiber birefringence has to be taken into account in the nonlinear broadening process, for a preserved polarization leads to enhanced nonlinear interactions so less power is required to generate SC. Lehtonen et al. [44] demonstrated the possibility of generating SC in a highly birefringent PCF in two orthogonal polarizations simultaneously. The two states of polarization presented different dispersion characteristics, and as such the SC in each polarization exhibited a different spectral profile. Both polarization states could be combined freely, thus adding an extra degree of freedom to the tuning of the final spectral properties.

The properties of highly-nonlinear germanosilicate (HNLF) fibers make them interesting nonlinear broadening media to be used in SC sources. As with microstructure fibers, the small effective area allows the fiber to be shortened even to the order of centimeters [155], and in addition, their nonlinear and dispersion properties can be more-or-less easily altered by a series of post-processing techniques, such as tapering [97] and UV irradiation [156]. This allows for a greater flexibility in the design of SC sources. A proper dispersion profile of the fiber can lead to the generation of a broader SC or one with lower relative intensity noise. UV irradiation is not the only available method for varying the dispersion properties of a fiber, and other possibilities, such as the immersion of tapered fibers in different liquids, have been studied with the idea of making them more suitable for the generation of SC [157]. In a recent contribution, Westbrook et al. [158] demonstrated that SC generation is greatly modified in the presence of fiber Bragg gratings, and reported enhancements of more than ten times in fibers with single and multiple grating resonances. Pre-shaping of the input pulse in a fiber Bragg grating prior to its broadening by SPM in a highly nonlinear fiber has also recently been suggested and demonstrated by Almeida et al. [159] as an interesting alternative for generating ultra-flat SC. The idea derives from the behaviour of the broadened spectrum of parabolic pulses [160].

4.1. Supercontinuum generation using dual-core air-clad fiber

In this section we focus on SC generation using special design of highly nonlinear tapered fiber. Advantage of a relatively simple fabrication process for tapered fiber can be combined with a reasonable design freedom using a dual-core tapered fiber (DCTF). The dual-core tapered design of highly nonlinear fiber allows a simple fabrication procedure leading to low cost for such a device. Compact design is advantageous for packaging. SMF-compatible input and output ports provide high splicing efficiency. Dual-core configuration makes possible richer and more flexible design possibilities compared to conventional cylindrical tapered fibers. Dual-core tapered fiber has been manufactured by drawing a pair of stripped SMFs. During the draw process the cross-section profile of the fiber can be changed from a figure-of-eight shape to quasi-elliptic. A formed fused dual-core waveguide has two input ports and two output ports, which makes possible its application as a coupler. It is smoothly tapered to the input and output ports that retain a structure of original SMFs. We discuss now in more detail an experiment on SC generation in DCTF.

4.1.1. Flexibility of DCTF design

A new degree of freedom (the core separation) of DCTF determines fiber geometry and can be used for better control of the SC generation process. A dual-core fiber is essentially multi-mode because of high contrast between the glass core and air cladding. However it is possible to design a dual core configuration so that only one mode is efficiently excited. A dual-core fiber configuration is characterized by the core diameter b and distance between the core centers a, or aspect ratio b/a. It is possible to tune the fiber geometry so that the light coming into one of the input ports can be efficiently coupled to only one of the waveguide modes. In the considered configuration a launched laser beam excites as asymmetric dipole mode.

Figures 2 and 3 show dispersion of the dipole anti-symmetric mode that is exited in the DCTF. An important feature of the dual core design is the possibility of tuning the zero dispersion point (ZDP) (shown by the bold line in Fig. 2) by variation of waveguide

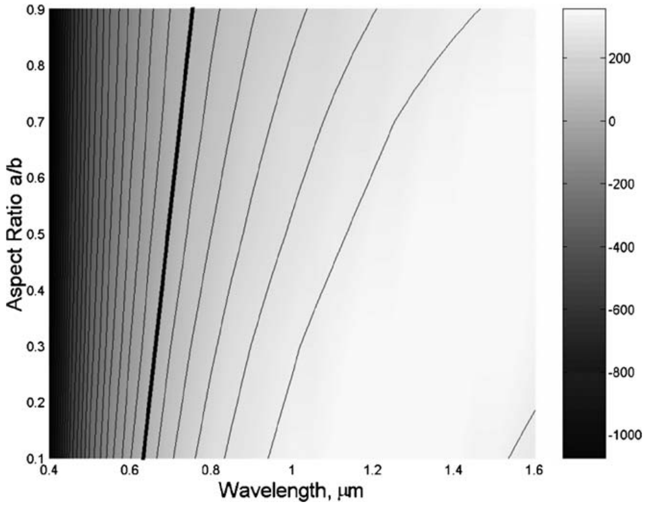

Fig. 2. Contour plot of dispersion of silica–air clad fiber for different aspect ratios ($b = 2$ μm). Bold line—ZDP.

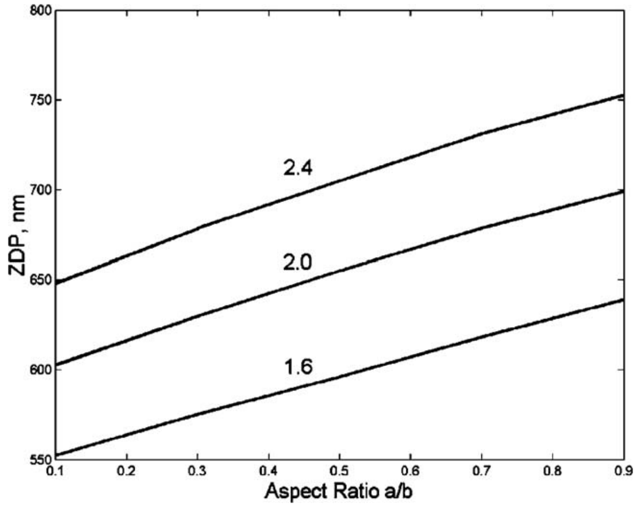

Fig. 3. Zero dispersion point versus aspect ratio a/b for different core diameters (labelled).

parameters. Several general properties can be observed. Smaller core diameter and larger distance between the cores correspond to higher dispersion. Another distinctive property is a noticeable shift of zero the dispersion wavelength with variations of the core diameter.

4.1.2. Experimental setup and results

The experimental setup shown in Fig. 4 comprises a Ti:Sapphire femtosecond laser source followed by the double-prism pair to provide optimal pre-chirping for SC generation in the DCTF. The SC generation takes place in a uniform section in the middle of the DCTF

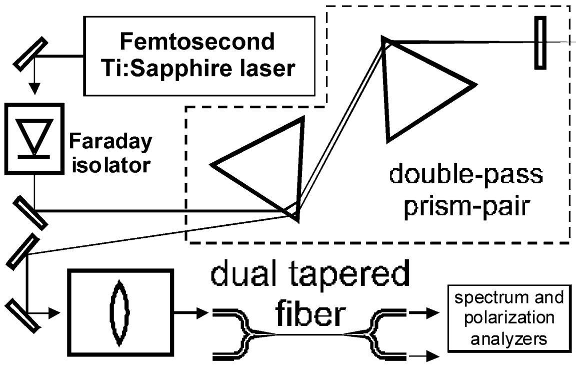

Fig. 4. Experimental setup.

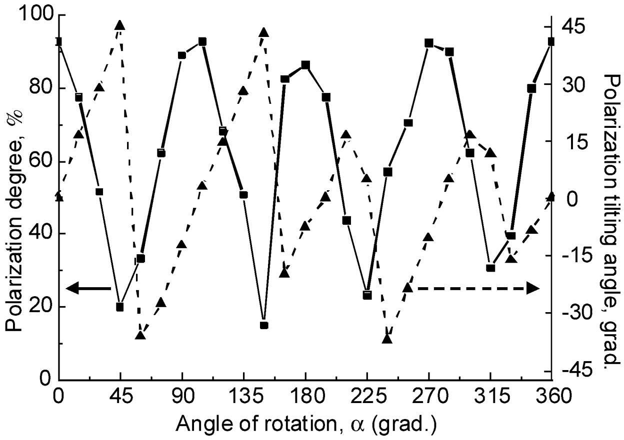

Fig. 5. Polarization properties of generated SC.

because it has the smallest effective area throughout the device. This waveguide also has a controllable dispersion provided by the anti-symmetric dipole mode as described below.

It has been observed that SC is initiated at a certain point in dual-core fiber. Typically, this point is at 2 cm after the input taper to get the widest output spectrum and is controlled by the initial pre-chirp. Another important observation is that the two output beams have the same peak power. It implicitly confirms the generation of the dipole single mode inside the dual core waist section of this device, because the equal partition of power between two output ports does not depend on the waist length. Both output light beams have practically Gaussian profile and are polarized along the major axes.

Polarization properties of the generated SC are illustrated in Fig. 5. Solid curve shows the degree of polarization of SC (%) versus the angle α between input polarization plane and major axis of dual core waveguide. The degree of polarization δ is determined from the results of measurement of maximal ($I_{\max}$) and minimal ($I_{\min}$) SC intensities passing through the rotating polarizer (Glan prism) by the formula: $\delta(\%) = 100 \times (I_{\max} - I_{\min})/(I_{\max} + I_{\min})$. The dashed curve shows the SC polarization tilting angle versus α.

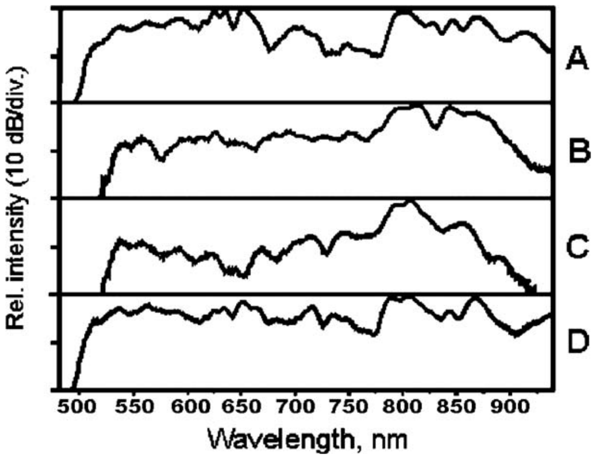

Fig. 6. Super-continuum spectra for different degrees of polarization: A: $\delta = 93\%$ ($\alpha = 0°$), B: $\delta = 68\%$ ($\alpha = 120°$), C: $\delta = 23\%$ ($\alpha = 225°$), D: $\delta = 93\%$ ($\alpha = 270°$).

Figure 6 shows the spectrum of generated SC. It is seen that the output spectra of polarized SC cover over 400 nm at the −20 dB level.

5. Nonlinear broadening of continuous wave sources

As we have shown, nonlinear broadening is usually achieved by transmitting short, high-power pulses through a strongly nonlinear medium. The initial modulation leads to an increased initial bandwidth and allows for the effect of SPM to act on the transmitted signal from the beginning, usually increasing the efficiency of the broadening process. On occasion, however, it can be practical to generate a wide spectrum from a conventional high-power CW source (typically a fiber laser). This possibility was illustrated in 2000 by the work of Prabhu et al. [161], who demonstrated the generation of a 100 nm SC centered at 1483.4 nm with output power of over 1 W and a weak spectral modulation of 0.11 nm, from a 1064 nm CW 8.4 W yterbium-doped fiber laser. The broadening medium was comprised of 700 m phosphorus-doped and 500 m Flexcor-1060 single-mode fiber that, together with a series of gratings, formed a Raman and a Brillouin cavity. The whole setup worked as an hybrid Raman–Brillouin fiber laser that produced a broad output SC spectrum. Further work on this direction was carried out by Abeeluck et al. [112,162], who in 2003 demonstrated the generation of a broad 247 nm SC by pumping a 4.5 km HNLF with a tunable Raman fiber laser, and clearly identified modulational instability (MI) as a fundamental effect in the generation of the SC. The same authors have recently reported much broader SC generation of more than 544 nm bandwidth, with output powers of up to 3.2 W [115,163]. Other groups have made recent contributions to the use of CW to generate SC. González-Herráez et al. [113] showed that CW-generated SC could be effectively used to perform accurate, long-range (>200 km) measurements of polarization mode dispersion in fibers.

5.1. Nonlinear pump broadening for Raman amplification

Nonlinear broadening can also be applied to the pumps of a Raman amplifier, in order to reduce its gain ripple when amplifying over a large bandwidth. The gain ripple in broadband Raman amplification can also be minimized by using a large number of pumps, but this is not always a practical solution, since it implies an increase on the complexity of the system, reducing its adaptability and increasing its cost. A Raman pump can be initially modulated and then rapidly broadened through SPM, but a more interesting possibility is to use modulational instability in the fiber to provide the initial modulation, thus considerably simplifying the design of the amplifier by using continuous wave pump lasers. This was the approach originally taken by Ellingham et al. [164], and later followed by Chestnut et al. [165] to broaden the spectra of single pumps in different sets of fiber. In Ellingham et al.'s original paper, the broadening performance of several non-zero dispersion-shifted fibers was evaluated for different pump input powers, and a five-fold gain ripple reduction was predicted for future dual-pump implementations. In order to maximize the effect of modulational instability, the wavelengths of the pumps must be such that they propagate through the broadening fiber in the slightly anomalous regime, close to the zero-dispersion point. Other desirable properties of the fiber include a high nonlinear coefficient and a small attenuation, in order to minimize the power loss of the pump. The nonlinear-broadening method was finally applied to a multi-pump Raman amplifier by Ellingham et al. [166], using Truewave fiber, and increasing the 0.1 dB gain ripple bandwidth from 5 to 19 nm in an amplifier designed to provide gain in the 1565–1595 nm region.

5.1.1. Setup and basic theory for Raman amplification with nonlinearly broadened pumps

Figure 7 (after [166]) depicts a traditional transmission line, backward-pumped with two conventional laser pumps, centered at 1455 and 1480 nm, respectively.

Each of the pumps propagates through a different broadening pre-fiber before being combined together by a 3 dB coupler and then injected into the transmission/amplification medium via a WDM. The WDM not only couples the pump light into the transmission line but also removes any spontaneous component that may otherwise occupy the signal band.

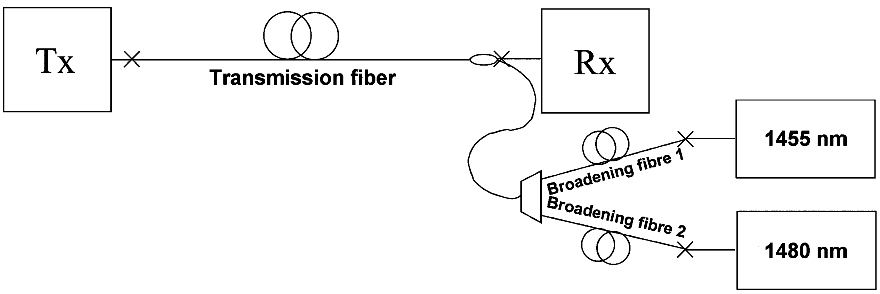

Fig. 7. Nonlinearly-broadened, dual-pump amplifier system schematic.

In the first stages of nonlinear broadening, in which MI is the dominating effect, the frequency-dependent gain coefficient, under the assumption of a coherent pump (which is enough for the purpose of this explanation), is given by the well-known expression

$$g(\Omega) = |\beta_2 \Omega| \left[\Omega_c^2 - \Omega^2\right]^{1/2}. \tag{3}$$

Obviously, the gain exists only if

$$\Omega^2 < \Omega_c^2 = \left(4\gamma P_{in} e^{-\alpha z}\right) / |\beta_2|, \tag{4}$$

where γ is the fiber nonlinear coefficient, β_2 is the dispersion, α is the fiber loss, and P_{in} is the pump input power. The MI causes power transfer from the CW pump and generates two bands symmetrically positioned at both sides of the initial pump, with a maximum at

$$\omega_0 \pm \Omega_{max} = \left[2\gamma P_{in} \exp(-\alpha z)/|\beta_2|\right]^{1/2}. \tag{5}$$

In the time domain, the CW beam is converted into a periodic pulse train with the period $T = 2\pi/\Omega_{max}$. The separation of the side peaks depends on the characteristics of the fiber. A low (but anomalous) dispersion leads to a more substantial broadening. Therefore, a simple design rule is to choose pump/fiber parameters using the expression for Ω_{max} in order to shift the side peaks to the required positions in the spectral domain. The dependence of MI characteristics on input power, dispersion and nonlinear coefficient can be used to select the best combination of pump/fiber parameters in order to achieve optimal pump broadening at any given frequency. Please note that although the simple analytical approximation used in Eqs. (3)–(5) is sufficient for our purpose of illustrating the initial break-up mechanism of the continuous wave beam, a precise analysis of the MI process in realistic conditions would have to account both for the fiber loss in a nonphenomenological way [167] and for the partial coherence of the pump sources, as illustrated in [168,169].

MI is the dominant effect on the initial stages of the pump broadening only, and the final spectrum of the broadened pump will be defined by the interplay between the various nonlinear effects on the fiber. Nevertheless, the necessary conditions for MI initiation set fundamental requirements on pump/fiber parameters, as illustrated by the results of experimental tests presented in Fig. 8, which shows the variation of the −10 dB m bandwidth of 900 mW CW pump transmitted through 25 km truewave reels with slightly different dispersion values. The dispersion was varied by using different reels and operating temperatures.

5.1.2. Effects of nonlinear broadening on the amplifier gain

Figure 9 gives an idea of the improvements that can be obtained by using this method. In this case, two truewave-RS fibers were used for the broadening of the pumping waves. For the 1455 nm pump, a 10.390 km reel with a zero-dispersion wavelength of approximately 1454 nm and a dispersion slope of 0.046 $\text{ps/nm}^2/\text{km}$ was used. The 1480 nm pump was broadened in a 5.077 km piece of fiber with zero dispersion wavelength at approximately 1475 nm with a dispersion slope of 0.049 $\text{ps/nm}^2/\text{km}$. The nonlinear coefficient of truewave (given at 1550 nm) is 1.84 $\text{W}^{-1}\text{km}^{-1}$. The transmission/amplification fiber was a 25.26 km E-LEAF reel. Due to the fact of the broadening fibers not being ideal, the broadened spectra are asymmetric, causing a noticeable offset of the effective central wavelength of the pumps at high powers. Both the broadening and the offset are less evident for

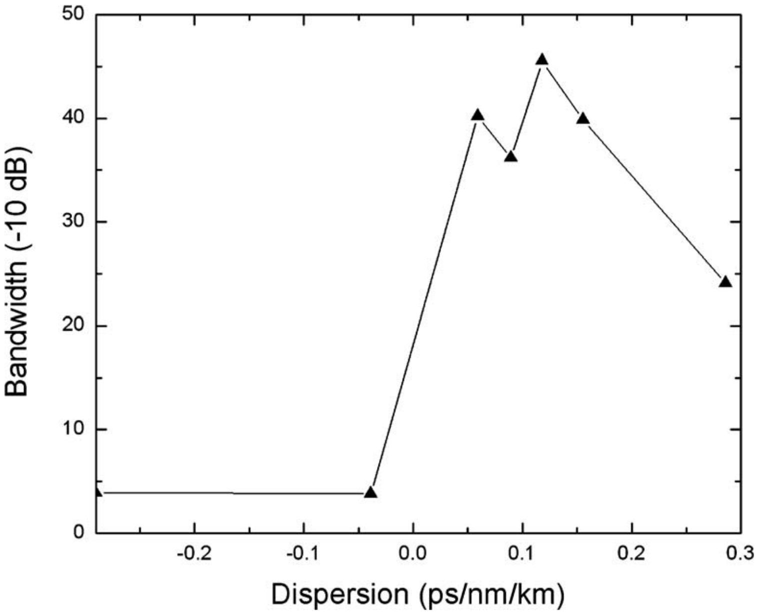

Fig. 8. Experimental −10 dB m bandwidth (in nm) for different low dispersion values.

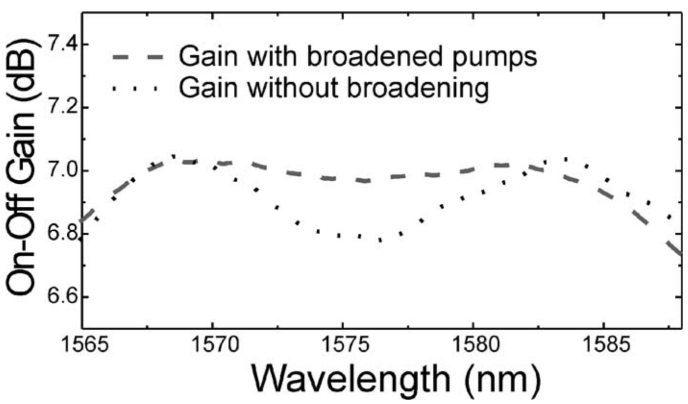

Fig. 9. Comparison between the gain ripples with and without pump broadening.

the 1480 nm pump, which is more than 5 nm apart from the zero-dispersion wavelength of its broadening fiber and has a shorter length. Even though these led to a drop in the gain at about 1590 nm for the broadened pump amplifier, the improvements in gain ripple performance are evident, as shown in Fig. 9. In particular, the continuous bandwidth corresponding to a gain ripple of 0.1 dB is increased from 5 to 19 nm, and the total gain variation over a 20 nm window is halved from 0.26 to 0.13 dB. The integrated pump powers of the broadened pumps used were 391 mW (1455 nm) and 715 mW (1480 nm), from input powers of 690 and 1052 mW, respectively. Further losses in the coupler between the broadening fibers and the transmission fiber will bring the pump powers down to 190 mW (1455 nm) and 290 mW (1480 nm) at the input of the transmission fiber.

This example illustrates the possibility of applying the broadening technique to multi-wavelength Raman amplifier design, but also shows that an improvement of the degree of broadening and a reduction of the pump power losses in the 'pre-fiber' are required to obtain a more viable solution. Utilizing fibers with more appropriate nonlinear/dispersive characteristics such as HNLF can be the best way of achieving this goal.

6. Conclusions

In this paper we have overviewed applications of nonlinear spectral broadening in telecommunications such as: multi-wavelength optical sources, TDM-WDM-TDM conversion, Raman amplifiers and others. While we have done our best to be thorough and fair towards all publications cited in our paper, the reader will obviously detect an intentional bias in terms of the space and detail dedicated towards those topics with which we are particularly familiarized and involved. This is not at all to imply a higher relative importance of such topics in comparison with the rest of the subjects discussed on the review, but instead should be considered as an attempt to provide additional detail on specific examples of nonlinear broadening applications whenever our proximity to the subject has allowed us to do so.

A large number of experimental and theoretical studies of SC properties and the peculiarities of nonlinear broadening in various media and conditions have been published in recent years. However we would like to emphasize that in spite of the significant progress in the development of SC sources and successful application of theoretical models to optimize the generation of broad radiation sources, the comprehension of the complex nonlinear mechanism of CG is not complete, and future development of these investigations is directly related to further improvement of the aforementioned models. At the present time, a quantitative agreement between experimental and numerical simulation results of CG is rather an exception than the norm. Furthermore, in the recent publications on CG both with pulsed [96,116] and CW [112] pumps, the authors pointed out some qualitative discrepancies between experimental results and theoretical predictions. Many questions remain unanswered, and the great potential for further improvement of our understanding of these remarkable scientific problems, along with the impressive range of interesting practical applications of SC are the main factors that make the field so exciting and attractive.

Acknowledgments

This work was supported by the INTAS (Grants 03-56-203 and 03-51-5288) and NATO Collaborative Linkage Grant PST.CLG.980074.

References

[1] J.C. Knight, T.A. Birks, P.S. Russell, D.M. Atkin , All-silica single-mode optical fiber with photonic crystal cladding, Opt. Lett. 21 (19) (1996) 1547–1549.

[2] J.Y.Y. Leong, P. Petropoulos, S. Asimakis, H. Ebendorff-Heidepriem, R.C. Moore, K. Frampton, V. Finazzi, X. Feng, J.H. Price, T.M. Monro, D.J. Richardson, A lead silicate holey fiber with $\gamma = 1820\ \mathrm{W}^{-1}\,\mathrm{km}^{-1}$ at 1550 nm, in: Proceedings of OFC 2005, Anaheim, 2005.
[3] R. Holzwarth, T. Udem, T.W. Hansch, J.C. Knight, W.J. Wadsworth, P.S.J. Russell, Optical frequency synthesizer for precision spectroscopy, Phys. Rev. Lett. 85 (2000) 2264–2267.
[4] A.B. Fedotov, A.M. Zheltikov, A.A. Ivanov, M.V. Alfimov, D. Chorvat, V.I. Beloglazov, L.A. Melnikov, N.B. Skibina, A.P. Tarasevitch, D. von der Linde, Supercontinuum-generating holey fibers as new broadband sources for spectroscopic applications, Laser Phys. 10 (2000) 723–726.
[5] G.S. He, T.C. Lin, P.N. Prasad, New technique for degenerate two-photon absorption spectral measurements using femtosecond continuum generation, Opt. Express 10 (2002) 566–574.
[6] S.T. Sanders, Wavelength-agile fiber laser using group-velocity dispersion of pulsed super-continua and application to broadband absorption spectroscopy, Appl. Phys. B Lasers Opt. 75 (2002) 799–802.
[7] I. Hartl, X.D. Li, C. Chudoba, R.K. Ghanta, T.H. Ko, J.G. Fujimoto, J.K. Ranka, R.S. Windeler, Ultrahigh-resolution optical coherence tomography using continuum generation in an air–silica microstructure optical fiber, Opt. Lett. 26 (2001) 608–610.
[8] A.A. Ivanov, M.V. Alfimov, A.B. Fedotov, A.A. Podshivalov, D. Chorvat, A.M. Zheltikov, An all-solid-state sub-40-fs self-starting Cr^{4+}: Forsterite laser with holey-fiber beam delivery and chirp control for coherence-domain and nonlinear-optical biomedical applications, Laser Phys. 11 (2001) 158–163.
[9] B. Povazay, K. Bizheva, A. Unterhuber, B. Hermann, H. Sattmann, A.F. Fercher, W. Drexler, A. Apolonski, W.J. Wadsworth, J.C. Knight, P.S.J. Russell, M. Vetterlein, E. Scherzer, Submicrometer axial resolution optical coherence tomography, Opt. Lett. 27 (2002) 1800–1802.
[10] Y.M. Wang, Y.H. Zhao, J.S. Nelson, Z.P. Chen, R.S. Windeler, Ultrahigh-resolution optical coherence tomography by broadband continuum generation from a photonic crystal fiber, Opt. Lett. 28 (2003) 182–184.
[11] D.L. Marks, A.L. Oldenburg, J.J. Reynolds, S.A. Boppart, Study of an ultrahigh-numerical-aperture fiber continuum generation source for optical coherence tomography, Opt. Lett. 27 (2002) 2010–2012.
[12] D.J. Kane, R. Trebino, Single-shot measurement of the intensity and phase of an arbitrary ultrashort pulse by using frequency-resolved optical gating, Opt. Lett. 18 (1993) 823–825.
[13] J. Dudley, X. Gu, L. Xu, M. Kimmel, E. Zeek, P. O'Shea, R. Trebino, S. Coen, R. Windeler, Cross-correlation frequency resolved optical gating analysis of broadband continuum generation in photonic crystal fiber: Simulations and experiments, Opt. Express 10 (2002) 1215–1221.
[14] X. Gu, L. Xu, M. Kimmel, E. Zeek, P. O'Shea, A.P. Shreenath, R. Trebino, R.S. Windeler, Frequency-resolved optical gating and single-shot spectral measurements reveal fine structure in microstructure-fiber continuum, Opt. Lett. 27 (2002) 1174.
[15] Q. Cao, X. Gu, E. Zeek, M. Kimmel, R. Trebino, J. Dudley, R.S. Windeler, Measurement of the intensity and phase of supercontinuum from an 8-mm-long microstructure fiber, Appl. Phys. B 77 (2003) 239–244.
[16] C. Iaconis, I.A. Walmsley, Spectral phase interferometry for direct electric-field reconstruction of ultrashort optical pulses, Opt. Lett. 23 (1998) 792–794.
[17] C. Iaconis, I.A. Walmsley, Self-referencing spectral interferometry for measuring ultrashort optical pulses, IEEE J. Quantum Electron. 35 (1999) 501–509.
[18] M.E. Anderson, L.E.E. de Araujo, E.M. Kosik, I.A. Walmsley, The effects of noise on ultrashort optical-pulse measurement using SPIDER, Appl. Phys. B 70 (2000) S85–S93.
[19] G. Stibenz, G. Steinmeyer, High dynamic range characterization of ultrabroadband white-light continuum pulses, Opt. Express 12 (2004) 6319–6325.
[20] K. Tamura, H. Kubota, M. Nakazawa, Fundamentals of Stable Continuum Generation at High Repetition Rates, IEEE J. Quantum. Electron. 36 (7) (2000) 773–779.
[21] Appl. Phys. B 77 (2–3) (2003), special issue.
[22] F. Biancalana, D.V. Skryabin, P.S. Russel, Four wave mixing instabilities in photonic-crystal and tapered fibers, Phys. Rev. E 68 (2003) 046631–046638.
[23] M.A. Foster, K.D. Moll, A.L. Gaeta, Optimal waveguide dimensions for nonlinear interactions, Opt. Express 12 (2004) 2880–2887.
[24] J.K. Ranka, A.L. Gaeta, Breakdown of the slowly varying envelope approximation in the self-focusing of ultrashort pulses, Opt. Lett. 23 (1998) 534–536.

[25] J.M. Dudley, S. Coen, Coherence properties of supercontinuum spectra generated in photonic crystal and tapered optical fibers, Opt. Lett. 27 (2002) 1180–1182.
[26] K.L. Corwin, N.R. Newbury, J.M. Dudley, S. Coen, S.A. Diddams, K. Weber, R.S. Windeler, Fundamental noise limitations to supercontinuum generation in microstructure fiber, Phys. Rev. Lett. 90 (2003) 113,904.
[27] N.I. Nikolov, T. Sorensen, O. Bang, A. Bjarklev, Improving efficiency of supercontinuum generation in photonic crystal fibers by direct degenerate four-wave-mixing, J. Opt. Soc. Amer. B 11 (2003) 2329–2337.
[28] W.J. Wadsworth, A. Ortigosa-Blanch, J.C. Knight, T.A. Birks, T.P.M. Man, P.St.J. Russell, Supercontinuum generation in photonic crystal fibers and optical fiber tapers: a novel light source, J. Opt. Soc. Amer. B 19 (2002) 2148–2155.
[29] J.W. Nicholson, M.F. Yan, P. Wisk, J. Fleming, F. DiMarcello, E. Monberg, A. Yablon, C. Jørgensen, T. Veng, All-fiber, octave-spanning supercontinuum, Opt. Lett. 28 (2003) 643–645.
[30] J.W. Nicholson, P.S. Westbrook, K.S. Feder, A.D. Yablon, Supercontinuum generation in ultraviolet-irradiated fibers, Opt. Lett. 29 (2004) 2363–2365.
[31] J. Takanayagi, N. Nishizawa, H. Nagai, M. Yoshida, T. Goto, Generation of high-power femtosecond pulse and octave-spanning ultrabroad supercontinuum using all-fiber system, IEEE Photon. Technol. Lett. 17 (2005) 37–39.
[32] R.R. Alfano, S.L. Shapiro, Emission in the region 4000 to 7000 angstrom via four-photon coupling in glass, Phys. Rev. Lett. 24 (1970) 584–587.
[33] W.H. Reeves, D.V. Skryabin, F. Biancalana, J.C. Knight, P.S.J. Russell, F.G. Omenetto, A. Efimov, A.J. Taylor, Transformation and control of ultra-short pulses in dispersion-engineered photonic crystal fibres, Nature 424 (2003) 511–515.
[34] B.P. Nelson, D. Cotter, K.J. Blow, N.J. Doran, Large non-linear pulse broadening in long lengths of monomode fibre, Opt. Commun. 48 (1983) 292–294.
[35] P.L. Baldeck, R.R. Alfano, Intensity effects on the stimulated four photon spectra generated by picosecond pulses in optical fibers, J. Lightwave Technol. 5 (1987) 1712–1715.
[36] J.K. Ranka, R.S. Windeler, A.J. Stentz, Efficient visible continuum generation in air–silica microstructure optical fibers with anomalous dispersion at 800 nm, in: Conference on Lasers and Electrooptics (CLEO '99), 1999, pp. CPD8/1–CPD8/2.
[37] J.K. Ranka, R.S. Windeler, A.J. Stentz, Visible continuum generation in air–silica microstructure optical fibers with anomalous dispersion at 800 nm, Opt. Lett. 25 (2000) 25–27.
[38] K. Mori, K. Takara, S. Kawanishi, The effect of pump fluctuation in supercontinuum pulse generation, OSA Tech. Dig. Ser. 5 (1998) 276–278.
[39] M. Nakazawa, K. Tamura, H. Kubota, E. Yoshida, Coherence degradation in the process of supercontinuum generation in an optical fiber, Opt. Fiber Technol. 4 (1998) 215–223.
[40] H. Kubota, K. Tamura, M. Nakazawa, Analyzes of coherence maintained ultrashort optical pulse trains and supercontinuum in the presence of soliton-amplified spontaneous-emission interaction, J. Opt. Soc. Amer. B 16 (1999) 2223–2232.
[41] K.L. Corwin, N.R. Newbury, J.M. Dudley, S. Coen, S.A. Diddams, B.R. Washburn, K. Weber, R.S. Windeler, Fundamental amplitude noise limitations to supercontinuum spectra generated in microstructure fiber, Appl. Phys. B 77 (2003) 269–277.
[42] B.R. Washburn, N.R. Newbury, Phase, timing, and amplitude noise on supercontinua generated in microstructure fiber, Opt. Express 12 (2004) 2166–2175.
[43] A. Proulx, J. Ménard, N. Hô, J.M. Laniel, R. Vallée, C. Paré, Intensity and polarization dependences of the supercontinuum generation in birefringent and highly nonlinear microstructured fibers, Opt. Express 11 (2003) 3338–3345.
[44] M. Lehtonen, G. Genty, H. Ludvigsen, M. Kaivola, Supercontinuum generation in a highly birefringent microstructured fiber, Appl. Phys. Lett. 82 (2003) 2197–2199.
[45] W. Drexler, U. Morgner, F.X. Kärtner, C. Pitris, S.A. Boppart, X.D. Li, E.P. Ippen, J.G. Fujimoto, In vivo ultrahigh-resolution optical coherence tomography, Opt. Lett. 24 (1999) 1221–1224.
[46] A.F. Fercher, W. Drexler, C.K. Hitzenberger, T. Lasser, Optical coherence tomography—principles and applications, Rep. Progr. Phys. 66 (2003) 239–303.
[47] Y.M. Wang, J.S. Nelson, Z.P. Chen, B.J. Reiser, R.S. Chuck, R.S. Windeler, Optimal wavelength for ultrahigh-resolution optical coherence tomography, Opt. Express 11 (2003) 1411–1417.
[48] W. Drexler, Ultrahigh-resolution optical coherence tomography, J. Biomed. Opt. 9 (2004) 47–74.

[49] D.A. Jones, S.A. Diddams, J.K. Ranka, A. Stentz, R.S. Windeler, J.L. Hall, S.T. Cundiff, Carrier-envelope phase control of femtosecond mode-locked lasers and direct optical frequency synthesis, Science 288 (2000) 635–639.

[50] S.A. Diddams, D.J. Jones, J. Ye, T. Cundiff, J.L. Hall, J.K. Ranka, R.S. Windeler, R. Holzwarth, T. Udem, T.W. Hänsch, Direct link between microwave and optical frequencies with a 300 THz femtosecond laser comb, Phys. Rev. Lett. 84 (2000) 5102–5105.

[51] M. Bellini, T.W. Hänsch, Phase-locked white-light continuum pulses: Toward a universal optical frequency-comb synthesizer, Opt. Lett. 25 (2000) 1049–1051.

[52] S.A. Diddams, D.J. Jones, J. Ye, T.M. Fortier, R.S. Windeler, S.T. Cundiff, T.W. Hänsch, J.L. Hall, Towards the ultimate control of light: Optical frequency metrology and the phase control of femtosecond pulses, Opt. Photon. News 11 (2000) 16–22.

[53] R. Holzwarth, M. Zimmermann, Th. Udem, T.W. Hänsch, A. Nevsky, J. von Zanthier, H. Walther, J.C. Knight, W.J. Wadsworth, P.St.J. Russell, M.N. Skvortsov, S.N. Bagayev, Absolute frequency measurement of iodine lines with a femtosecond optical synthesizer, Appl. Phys. B 73 (2001) 269–271.

[54] S.A. Diddams, D.J. Jones, J. Ye, S.T. Cundiff, J.L. Hall, J.K. Ranka, R.S. Windeler, Direct RF to optical frequency measurements with a femtosecond laser comb, IEEE Trans. Instrum. Meas. 50 (2001) 552–555.

[55] D. Wang, H. Jiang, S. Wu, H. Yang, Q. Gong, J. Xiang, G. Xu, An investigation of solvent effects on the optical properties of dye IR-140 using the pump supercontinuum-probing technique, J. Opt. A Pure Appl. Opt. 5 (2003) 515–519.

[56] R.R. Alfano, S.L. Shapiro, Observation of self-phase modulation and small-scale filaments in crystals and glasses, Phys. Rev. Lett. 24 (1970) 592–594.

[57] G.P. Agrawal, Nonlinear Fiber Optics, Academic Press, San Diego, 2001.

[58] N. Bloembergen, The influence of electron plasma formation on superbroadening in light filaments, Opt. Commun. 8 (1973) 285–288.

[59] W. Werncke, A. Lau, M. Pfeiffer, K. Lenz, H.-J. Weigmann, C.D. Thuy, An anomalous frequency broadening in water, Opt. Commun. 4 (1972) 413–415.

[60] W.L. Smith, P. Liu, N. Bloembergen, Superbroadening in H_2O and D_2O by self-focused picosecond pulses from a YAlG:Nd laser, Phys. Rev. A 15 (1977) 2396–2403.

[61] P.B. Corkum, C. Rolland, T. Srinivasan-Rao, Supercontinuum generation in gases, Phys. Rev. Lett. 57 (1986) 2268–2271.

[62] P.B. Corkum, C. Rolland, Femtosecond continua produced in gases, IEEE J. Quantum Electron. 25 (1989) 2634–2639.

[63] V. François, F.A. Ilkov, S.L. Chin, Experimental study of the supercontinuum spectral width evolution in CO_2 gas, Opt. Commun. 99 (1993) 241–246.

[64] C. Lin, R.H. Stolen, New nanosecond continuum for excited-state spectroscopy, Appl. Phys. Lett. 28 (1976) 216–218.

[65] P.L. Baldeck, R.R. Alfano, Intensity effects on the stimulated four photon spectra generated by picosecond pulses in optical fibers, J. Lightwave Technol. 5 (1987) 1712–1715.

[66] T. Morioka, K. Mori, M. Saruwatari, More than 100-wavelength-channel picosecond optical pulse generation from single laser source using supercontinuum in optical fibers, Electron. Lett. 29 (1993) 862–864.

[67] R.A. Fisher, P.L. Kelley, T.K. Gustafson, Subpicosecond pulse generation using the optical Kerr effect, Appl. Phys. Lett. 14 (1969) 140.

[68] A.S. Gouveia-Neto, A.S.L. Gomes, J.R. Taylor, Generation of 33-fs pulses at 1.32 μm through a high-order soliton effect in a single-mode optical fiber, Opt. Lett. 12 (1987) 395–397.

[69] W.J. Tomlinson, R.J. Stolen, C.V. Shank, Compression of optical pulses chirped by self-phase modulation in fibers, J. Opt. Soc. Amer. B 1 (1984) 139–149.

[70] R.L. Fork, C.H. Brito Cruz, P.C. Becker, C.V. Shank, Compression of optical pulses to six femtoseconds by using cubic phase compensation, Opt. Lett. 12 (1987) 483–485.

[71] K. Tamura, M. Nakazawa, Timing jitter of solitons compressed in dispersion-decreasing fibers, Opt. Lett. 23 (1998) 1360–1362.

[72] K. Mori, H. Takara, S. Kawanishi, M. Saruwatari, T. Morioka, Flatly broadened supercontinuum generated in a dispersion decreasing fiber with convex dispersion profile, Electron. Lett. 33 (1997) 1806–1808.

[73] T. Okuno, M. Onishi, M. Nishimura, Generation of ultra-broad-band supercontinuum by dispersion-flattened and decreasing fiber, IEEE Photon. Technol. Lett. 10 (1998) 72–74.

[74] K. Mori, H. Takara, S. Kawanishi, Analysis and design of supercontinuum pulse generation in a single-mode optical fiber, J. Opt. Soc. Amer. B 18 (2001) 1780–1792.

[75] J.C. Knight, T.A. Birks, P.S.J. Russell, D.M. Atkin, All-silica single-mode optical fiber with photonic crystal cladding, Opt. Lett. 21 (1996) 1547–1549.

[76] J.C. Knight, T.A. Birks, P.S.J. Russell, D.M. Atkin, All-silica single-mode optical fiber with photonic crystal cladding: Errata, Opt. Lett. 22 (1997) 484–485.

[77] T.A. Birks, J.C. Knight, P.S.J. Russell, Endlessly single-mode photonic crystal fiber, Opt. Lett. 22 (1997) 961–963.

[78] J. Broeng, S.E. Barkou, A. Bjarklev, J.C. Knight, T.A. Birks, P.S.J. Russell, Highly increased photonic band gaps in silica/air structures, Opt. Commun. 156 (1998) 240–244.

[79] J.C. Knight, T.A. Birks, P.S.J. Russell, J.P. de Sandro, Properties of photonic crystal fiber and the effective index model, J. Opt. Soc. Amer. A Opt. Image Sci. Vision 15 (1998) 748–752.

[80] J.C. Knight, T.A. Birks, R.F. Cregan, P.S.J. Russell, J.P. de Sandro, Large mode area photonic crystal fibre, Electron. Lett. 34 (1998) 1347–1348.

[81] J.C. Knight, J. Broeng, T.A. Birks, P.S.J. Russel, Photonic band cap guidance in optical fibers, Science 282 (1998) 1476–1478.

[82] D. Mogilevtsev, T.A. Birks, P.S.J. Russell, Group-velocity dispersion in photonic crystal fibers, Opt. Lett. 23 (1998) 1662–1664.

[83] E. Silvestre, P.S.J. Russell, T.A. Birks, J.C. Knight, Analysis and design of an endlessly single-mode finned dielectric waveguide, J. Opt. Soc. Amer. A Opt. Image Sci. Vision 15 (1998) 3067–3075.

[84] A.M. Zheltikov, Holey Fibers, in: Uspekhi Fizicheskikh Nauk, vol. 43, Russian Acad. Sci., 2000, pp. 1125–1136.

[85] R.F. Cregan, B.J. Mangan, J.C. Knight, Single-mode photonic and gap guidance of light in air, Science 285 (1999) 1537–1539.

[86] A. Ferrando, E. Silvestre, J.J. Miret, J.A. Monsoriu, M.V. Andres, P.S.J. Russell, Designing a photonic crystal fibre with flattened chromatic dispersion, Electron. Lett. 35 (1999) 325–327.

[87] A. Ferrando, E. Silvestre, J.J. Miret, P. Andres, Nearly zero ultraflattened dispersion in photonic crystal fibers, Opt. Lett. 25 (2000) 790–792.

[88] A. Ferrando, E. Silvestre, P. Andres, J.J. Miret, M.V. Andres, Designing the properties of dispersion-flattened photonic crystal fibers, Opt. Express 9 (2001) 687–697.

[89] W.H. Reeves, J.C. Knight, P.S.J. Russell, P.J. Roberts, Demonstration of ultra-flattened dispersion in photonic crystal fibers, Opt. Express 10 (2002) 609–613.

[90] G. Renversez, B. Kuhlmey, R. McPhedran, Dispersion management with microstructured optical fibers: Ultraflattened chromatic dispersion with low losses, Opt. Lett. 28 (2003) 989–991.

[91] K. Saitoh, M. Koshiba, T. Hasegawa, E. Sasaoka, Chromatic dispersion control in photonic crystal fibers: Application to ultra-flattened dispersion, Opt. Express 11 (2003) 843–852.

[92] F. Poli, A. Cucinotta, S. Selleri, A.H. Bouk, Tailoring of flattened dispersion in highly nonlinear photonic crystal fibers, IEEE Photon. Technol. Lett. 16 (2004) 1065–1067.

[93] K. Saitoh, M. Koshiba, Highly nonlinear dispersion-flattened photonic crystal fibers for supercontinuum generation in a telecommunication window, Opt. Express 12 (2004) 2027–2032.

[94] J.C. Knight, J. Arriaga, T.A. Birks, A. Ortigosa-Blanch, W.J. Wadsworth, P.S.J. Russell, Anomalous dispersion in photonic crystal fiber, IEEE Photon. Technol. Lett. 12 (2000) 807–809.

[95] J.K. Ranka, R.S. Windeler, A.J. Stentz, Optical properties of high-delta air–silica microstructure optical fibers, Opt. Lett. 25 (2000) 796–798.

[96] A. Apolonski, B. Povazay, A. Unterhuber, W. Drexler, W.J. Wadsworth, J.C. Knight, P.S.J. Russell, Spectral shaping of supercontinuum in a cobweb photonic-crystal fiber with sub-20-fs pulses, J. Opt. Soc. Amer. B 19 (2002) 2165–2170.

[97] T.A. Birks, W.J. Wadsworth, P.S.J. Russell, Supercontinuum generation in tapered fibers, Opt. Lett. 25 (2000) 1415–1417.

[98] D.A. Akimov, A.A. Ivanov, M.V. Alfimov, S.N. Bagayev, T.A. Birks, W.J. Wadsworth, P.S.J. Russell, A.B. Fedotov, V.S. Pivtsov, A.A. Podshivalov, A.M. Zheltikov, Two-octave spectral broadening of subnanojoule Cr:forsterite femtosecond laser pulses in tapered fibers, Appl. Phys. B 74 (2002) 307–311.

[99] S.M. Kobtsev, S.V. Kukarin, N.V. Fateev, S.V. Smirnov, Generation of self-frequency-shifted solitons in tapered fibers in the presence of femtosecond pumping, Laser Phys. 14 (2004) 748–751.

[100] A. Ortigosa-Blanch, J.C. Knight, P.S.J. Russell, Pulse breaking and supercontinuum generation with 200-fs pump pulses in PCF, J. Opt. Soc. Amer. B 19 (2002) 2567–2572.
[101] G. Genty, M. Lehtonen, H. Ludvigsen, J. Broeng, M. Kaivola, Spectral broadening of femtosecond pulses into continuum generation in microstructured fibers, Opt. Express 10 (2002) 1083–1098.
[102] A.V. Husakou, J. Herrmann, Supercontinuum generation of higher-order solitons by fission in photonic crystal fibers, Phys. Rev. Lett. 87 (2001) 203,901.
[103] J. Herrmann, U. Griebner, N. Zhavoronkov, A. Husakou, D. Nickel, J.C. Knight, W.J. Wadsworth, P.S.J. Russell, G. Korn, Experimental evidence for supercontinuum generation by fission of higher-order solitons in photonic fibers, Phys. Rev. Lett. 88 (2002) 173,901.
[104] J.P. Gordon, Theory of the soliton self-frequency shift, Opt. Lett. 11 (1986) 662–664.
[105] F.M. Mitschke, L.F. Mollenauer, Discovery of the soliton self-frequency shift, Opt. Lett. 11 (1986) 659–661.
[106] D.T. Reid, I.G. Cormack, W.J. Wadsworth, J.C. Knight, P.S.J. Russell, Soliton self-frequency shift effects in photonic crystal fibre, J. Modern Opt. 49 (2002) 757–767.
[107] J.M. Dudley, L. Provino, N. Grossard, H. Maillotte, R.S. Windeler, B.J. Eggleton, S. Coen, Supercontinuum generation in air–silica microstructured fiber with nanosecond and femtosecond pulse pumping, J. Opt. Soc. Amer. B 19 (2002) 765–771.
[108] S. Coen, A.H.L. Chau, R. Leonhardt, J.D. Harvey, J.C. Knight, W.J. Wadsworth, P.S.J. Russell, Supercontinuum generation by stimulated Raman scattering and parametric four-wave mixing in photonic crystal fibers, J. Opt. Soc. Amer. B 19 (2002) 753–764.
[109] S. Coen, A.H.L. Chau, R. Leonhardt, J.D. Harvey, J.C. Knight, W.J. Wadsworth, P.S.J. Russell, White-light supercontinuum generation with 60-ps pump pulses in a photonic crystal fiber, Opt. Lett. 26 (2001) 1356–1358.
[110] U. Morgner, F.X. Kärtner, S.H. Cho, Y. Chen, H.A. Haus, J.G. Fujimoto, E.P. Ippen, V. Scheuer, G. Angelow, T. Tschudi, Sub-two-cycle pulses from a Kerr-lens mode-locked Ti:sapphire laser, Opt. Lett. 24 (1999) 411–413.
[111] A. Bartels, H. Kurz, Generation of a broadband continuum by a Ti:sapphire femtosecond oscillator with a 1-GHz repetition rate, Opt. Lett. 27 (2002) 1839–1841.
[112] J.W. Nicholson, A.K. Abeeluck, C. Headley, M.F. Yan, C.G. Jørgensen, Pulsed and continuous-wave SC generation in highly nonlinear, dispersion-shifted fibers, Appl. Phys. B 77 (2003) 211–218.
[113] M. González-Herráez, S. Martín-López, P. Corredera, M.L. Hernanz, P.R. Horche, Supercontinuum generation using a continuous-wave Raman fiber laser, Opt. Commun. 226 (2003) 323–328.
[114] A.V. Avdokhin, S.V. Popov, J.R. Taylor, Continuous-wave, high-power Raman continuum generation in holey fibers, Opt. Lett. 28 (2003) 1353–1355.
[115] A.K. Abeeluck, C. Headley, C.G. Jørgensen, High-power supercontinuum generation in highly nonlinear, dispersion-shifted fibers by use of a continuous-wave Raman fiber laser, Opt. Lett. 29 (2004) 2163–2165.
[116] J. Teipel, K. Franke, D. Turke, F. Warken, D. Meiser, M. Leuschner, H. Giessen, Characteristics of supercontinuum generation in tapered fibers using femtosecond laser pulses, Appl. Phys. B 77 (2003) 245–251.
[117] M. Tianprateep, J. Tada, T. Yamazaki, F. Kannari, Spectral-shape-controllable supercontinuum generation in microstructured fibers using adaptive pulse shaping technique, Jpn. J. Appl. Phys. 43 (2004) 8059–8063.
[118] S.M. Kobtsev, S.V. Smirnov, Optimization of temporal characteristics of supercontinuum generated in tapered air-clad fibers, in: Proc. SPIE, vol. 5480, 2004, pp. 64–71.
[119] S.N. Bagaev, V.I. Denisov, V.F. Zakhar'yash, V.M. Klement'ev, S.M. Kobtsev, S.A. Kuznetsov, S.V. Kukarin, V.S. Pivtsov, S.V. Smirnov, N.V. Fateev, Spectral and temporal characteristics of a supercontinuum in tapered optical fibres, IEEE J. Quantum Electron. 34 (2004) 1107–1115.
[120] J. Zeller, J. Jasapara, W. Rudolph, M. Sheik-Bahae, Spectro-temporal characterization of a femtosecond white-light continuum generation by transient-grating diffraction, Opt. Commun. 185 (2000) 133–137.
[121] S.M. Kobtsev, S.V. Kukarin, N.V. Fateev, Generation of a polarised supercontinuum in small-diameter quasi-elliptic fibres, IEEE J. Quantum Electron. 33 (2003) 1085–1088.
[122] A.L. Gaeta, Nonlinear propagation and continuum generation in microstructured optical fibers, Opt. Lett. 27 (2002) 924–926.

[123] B.S.M. Kobtsev, S.V. Kukarin, N.V. Fateev, S.V. Smirnov, Coherent, polarization and temporal properties of self-frequency shifted solitons generated in polarization-maintaining microstructured fibre, Appl. Phys., in press.

[124] M.N. Islam, G. Sucha, I. Bar-Joseph, M. Wegener, J.P. Gordon, D.S. Chemla, Femtosecond distributed soliton spectrum fibers, J. Opt. Soc. Amer. B 6 (1989) 1149–1158.

[125] C.V. Shank, R.L. Fork, R. Yen, R.H. Stolen, Compression of femtosecond optical pulses, Appl. Phys. Lett. 40 (9) (1982) 761.

[126] T. Südmeyer, F. Brunner, E. Innerhofer, R. Paschotta, K. Furusawa, J.C. Baggett, T.M. Monro, D.J. Richardson, U. Keller, Nonlinear femtosecond pulse compression at high average power levels by use of a large mode-area holey fiber, Opt. Lett. 28 (2003) 1951–1953.

[127] B. Schenkel, J. Biegert, U. Keller, C. Vozzi, M. Nisoli, G. Sansone, S. Stagira, S. De Silvestri, O. Svelto, Generation of 3.8-fs pulses from adaptive compression of a cascaded hollow fiber supercontinuum, Opt. Lett. 28 (2003) 1987–1989.

[128] J.M. Dudley, S. Coen, Fundamental limits to few-cycle pulse generation from compression of supercontinuum spectra generated in photonic crystal fiber, Opt. Express 12 (2004) 2423–2428.

[129] N. Nishizawa, T. Goto, Widely broadened super continuum generation using highly nonlinear dispersion shifted fibers and femtosecond fiber laser, Jpn. J. Appl. Phys. 40 (2001) L365–L367.

[130] J.W. Nicholson, J.M. Fini, J.-C. Bouteiller, J. Bromage, K. Brar, Stretched ultrashort pulses for high repetition rate swept-wavelength Raman pumping, J. Lightwave Technol. 22 (1) (2004) 71–78.

[131] T. Morioka, et al., 1 Tbit/s 100 Gbit/s 10 channel OTDM-WDM transmission using a single supercontinuum WDM source, Electron. Lett. 32 (10) (1996) 906.

[132] K. Tamura, E. Yoshida, M. Nakazawa, Generation of 10 GHz pulse trains at 16 wavelengths by spectrally slicing a high power femtosecond source, Electron. Lett. 32 (18) (1996) 1691.

[133] H. Sotobayashi, W. Chujo, A. Konishi, T. Ozeki, Wavelength-band generation and transmission of 3.24-Tbit/s (81-channel WDM×40-Gbit/s) carrier-suppressed return-to-zero format by use of a single supercontinuum source for frequency standardization, J. Opt. Soc. Amer. B 19 (11) (2002) 2803.

[134] R.R. Alfano (Ed.), The Super Continuum Laser Sources, Springer-Verlag, Berlin, 1989.

[135] T. Takara, T. Ohara, K. Mori, K. Sato, E. Yamada, K. Jinguji, Y. Inoue, T. Shibata, T. Morioka, K.-I. Sato, More than 1000 channel optical frequency chain generation from a single supercontinuum source with 12.5 GHz channel spacing, Electron. Lett. 36 (2000) 2089–2090.

[136] H. Takara, H. Masuda, K. Mori, K. Sato, Y. Inoue, T. Ohara, A. Mori, M. Kohtoku, Y. Miyamoto, T. Morioka, S. Kawanishi, 124 nm seamless bandwidth, 313 × 10 Gbit/s DWDM transmission, Electron. Lett. 39 (2003) 382–383.

[137] T. Ohara, H. Takara, T. Yamamoto, H. Masuda, T. Morioka, M. Abe, H. Takahashi, Over 1000 channel, 6.25 GHz-spaced ultra-DWDM transmission with supercontinuum multi-carrier source, in: Proceedings of OFC 2005, Anaheim, 2005, paper OWA6.

[138] H. Sotobayashi, W. Chujo, A. Konishi, T. Ozeki, Wavelength-band generation and transmission of 3.24-Tbit/s (81-channel WDM×40-Gbit/s) carrier-suppressed return-to-zero format by use of a single supercontinuum source for frequency standardization, J. Opt. Soc. Amer. B 19 (2002) 2803.

[139] S.V. Kartapoulos, M. Bouhiyate, Supercontinuum sources in CWDM applications with channel protection, in: Proceedings of OFC 2005, Anaheim, 2005, paper NTuH4.

[140] S. Oda, S. Okamoto, A. Maruta, A novel quantization scheme by slicing supercontinuum spectrum for all-optical analog-to-digital conversion, in: Proceedings of NLGW 2004, Toronto, Canada, 2004, paper TuB3.

[141] S. Oda, A. Maruta, Experimental demonstration of optical quantizer based on slicing supercontinuum spectrum for all-optical analog-to-digital conversion, in: Proceedings of ECOC 2004, Stockholm, Sweden, 2004, paper We4.P.084.

[142] S. Oda, A. Maruta, A novel quantization scheme by slicing supercontinuum spectrum for all optical analog-to-digital conversion, IEEE Photon. Technol. Lett. 17 (2005) 465–467.

[143] P.P. Ho, Q.Z. Wang, J. Chen, Q.D. Liu, R.R. Alfano, Ultrafast optical pulse digitization with unary spectrally encoded cross-phase modulation, Appl. Opt. 36 (1997) 3425–3429.

[144] S. Oda, A. Maruta, All-optical analog-to-digital conversion by slicing supercontinuum spectrum and switching with nonlinear optical loop mirror, in: Proceedings of OFC 2005, Anaheim, 2005, paper OThN3.

[145] H. Sotobayashi, W. Chujo, T. Ozeki, Bi-directional photonic conversion between 4×10 Gbit/s OTDM and WDM by optical time-gating wavelength interchange, in: Proceedings of OFC 2001, Anaheim, 2001, paper WM5.

[146] H. Sotobayashi, W. Chujo, K. Kitayama, Photonic gateway: TDM-to-WDM-to-TDM conversion and reconversion at 40 Gbit/s (4 channels $\times$ 10 Gbits/s), J. Opt. Soc. Amer. B 19 (11) (2002) 2810.

[147] K. Mori, T. Morioka, M. Saruwatari, Ultrawide spectral range group-velocity dispersion measurement utilizing supercontinuum in an optical fiber pumped by a 1.5 μm compact laser source, IEEE Trans. Instrum. Meas. 44 (1995) 712–715.

[148] Q. Ye, C. Xu, X. Liu, W.H. Knox, M.F. Yan, R.S. Windeler, B. Eggleton, Dispersion measurement of tapered air–silica microstructure fiber by white-light interferometry, Appl. Opt. 41 (2002) 4467–4470.

[149] J. Jasapara, T.H. Her, R. Bise, R. Windeler, D.J. DiGiovanni, Group-velocity dispersion measurements in a photonic bandgap fiber, J. Opt. Soc. Amer. B 20 (8) (2003) 1611–1615.

[150] K. Mori, H. Takara, S. Kawanishi, M. Saruwatari, T. Morioka, Flatly broadened supercontinuum spectrum generated in a dispersion decreasing fiber with convex dispersion profile, Electron. Lett. 33 (1997) 1806–1808.

[151] J. Nicholson, M. Yan, A. Yablon, P. Wisk, J. Fleming, F. DiMarcello, E. Monberg, A high coherence supercontinuum source at 1550 nm, in: Optical Fiber Communication Conference 2003, vol. 86, pp. 511–512.

[152] T. Hori, J. Takayanagi, N. Nishizawa, T. Goto, Flatly broadened, wideband and low noise supercontinuum generation in highly nonlinear hybrid fiber, Opt. Express 12 (2004) 317–324.

[153] S. Kobtsev, S. Kukarin, N. Fateev, S. Turitsyn, V. Mezentsev, Silica/air-clad dual-core tapered fiber for polarized supercontinuum generation, in: Optical Fiber Communication Conference 2003, vol. 86, 2003, pp. 689–690, paper FH4.

[154] X. Gu, M. Kimmel, A.P. Shreenath, R. Trebino, J.M. Dudley, S. Coen, R.S. Windeler, Experimental studies of the coherence of microstructure-fiber supercontinuum, Opt. Express 11 (2003) 2697–2703.

[155] B.R. Washburn, S.A. Diddams, N.R. Newbury, J.W. Nicholson, M.F. Yan, C.G. Jorgensen, Phase-locked, erbium-fiber-laser-based frequency comb in the near infrared, Opt. Lett. 29 (2004) 250–252.

[156] P.S. Westbrook, J.W. Nicholson, K. Feder, A.D. Yablon, UV Processing of Highly Nonlinear Fibers for Enhanced Supercontinuum Generation, in: Proceedings of OFC 2004, 2004, paper PDP27.

[157] R. Zhang, J. Teipel, X. Zhang, D. Nau, H. Giessen, Group velocity dispersion of tapered fibers immersed in different liquids, Opt. Express 12 (2004) 1700–1707.

[158] P.S. Westbrook, J.W. Nicholson, K.S. Feder, Y. Li, T. Brown, Enhanced supercontinuum generation near fibre Bragg grating resonances, in: Proceedings of OFC 2005, 2005, paper OThQ4.

[159] P.J. Almeida, P. Petropoulos, M. Ibsen, D.J. Richardson, Generation of ultra-flat SPM-broadened spectra in a highly nonlinear fiber using pulse pre-shaping in a fiber Bragg grating, in: Proceedings of OFC 2005, 2005, paper OThA4.

[160] M.E. Fermann, V.I. Kruglov, B.C. Thomsen, J.M. Dudley, J.D. Harvey, Self-similar propagation amplification of parabolic pulses in optical fibers, Phys. Rev. Lett. 84 (26) (2000) 6010–6013.

[161] M. Prabhu, N.S. Kim, K. Ueda, Ultra-broadband CW supercontinuum generation centered at 1483.4 nm from Brillouin–Raman fiber laser, Jpn. J. Appl. Phys. 39 (2000) L291–L293.

[162] A.K. Abeeluck, S. Radic, K. Brar, J.-C. Bouteiller, C. Headley, in: Optical Fiber Communication Conference (OFC 2003), vol. 86, 2003, pp. 561–562.

[163] A.K. Abeeluck, C. Headley, C.G. Jorgensen, A fiber-based, high-power supercontinuum light source, in: Optical Fiber Conference (OFC 2004), 2004, paper TuK5.

[164] T.J. Ellingham, L.M. Gleeson, N.J. Doran, Enhanced Raman amplifier performance using non-linear pump broadening, in: Proceedings of ECOC 2002, 2002, paper 4.1.3.

[165] D.A. Chestnut, J.R. Taylor, Gain-flattened fiber Raman amplifiers with nonlinearity-broadened pumps, Opt. Lett. (2003) 2294–2296.

[166] T.J. Ellingham, J.D. Ania-Castañón, S.K. Turitsyn, A. Pustovskikh, S. Kobtsev, M.P. Fedoruk, Dual-pump Raman amplification with increased flatness using modulation instability, Opt. Express 13 (2005) 1079–1084.

[167] M. Karlsson, Modulational instability in lossy optical fibers, J. Opt. Soc. Amer. B 12 (11) (1995) 2071–2077.

[168] D. Anderson, L. Helczynski-Wolf, M. Lisak, V. Semenov, Features of modulational instability of partially coherent light: Importance of the incoherence spectrum, Phys. Rev. E (2004) 025601.
[169] A. Mussot, E. Lantz, H. Maillotte, T. Sylvestre, S. Pitois, Spectral broadening of a partially coherent CW laser beam in single-mode optical fibers, Opt. Express (2004) 2838.